Kovove Mater. 48 2010 185–190
DOI: 10.4149/km_2010_3_185

Comparison of dynamic mechanical properties of non-superheated and superheated A357 alloys

M. N. Mazlee*, J. B. Shamsul, H. Kamarudin

School of Materials Engineering, Universiti Malaysia Perlis (UniMAP), Kompleks Pusat Pengajian Jejawi 2, Taman Muhibah, Jejawi, 02600 Arau, Perlis, Malaysia

Received 24 March 2009, received in revised form 2 December 2009, accepted 1 March 2010

Abstract

The influence of superheat treatment on the microstructure and dynamic mechanical properties of A357 alloys has been investigated. The study of microstructure was performed by optical microscope. Dynamic mechanical properties (storage modulus, loss modulus and damping capacity) were measured by the dynamic mechanical analyzer (DMA). Microstructure showed coarser and angular eutectic Si particles with larger α-Al dendrites in non-superheated A357 alloy. In contrast, finer and rounded eutectic Si particles together with smaller and preferably oriented α-Al dendrites have been observed in superheated A357 alloy. Dynamic mechanical properties showed an increasing trend of loss modulus and damping capacity, meanwhile a decreasing trend of storage modulus at elevated temperatures for superheated and non-superheated A357 alloys. The significant improvement of damping capacities has been observed at lower temperatures range (50 to 277 °C) and higher temperatures range (278 to 380 °C) in non-superheated A357 alloy and superheated A357 alloy, respectively. The high damping capacity of superheated A357 alloy has been ascribed to the grain boundary damping at elevated temperatures.

K e y w o r d s: A357, melt superheat treatment, grain boundary damping

1. Introduction

In the last few decades, Al-Si-Mg alloy is one of the commercially most used alloys in the automotive and aircraft industries, which is noted for its excellent combination of good castability and mechanical properties as well as good corrosion resistance and weldability [1–3]. Solidification process plays a pivotal role in determining the resulted physical and mechanical properties of the alloys. The solidification sequence of Al-Si-Mg alloy consists mainly of three phase transformations by referring to the cooling curves, namely the formation of aluminum dendrites (α-Al dendrites), the main binary eutectic reaction and the formation of ternary and/or quaternary eutectic phases such as Mg_2Si and/or Fe-bearing intermetallics [4].

Melt superheat treatment is the alternative non-chemical and thermal treatment that has been practically utilized for grain refinement to the molten metal in aluminum alloys [5, 6] and magnesium alloys [7, 8]. Superheat treatment combined with grain refiner in production of Al-Si alloys has been proven towards improving mechanical properties [6, 9, 10]. Grain refinement by an addition of grain refiner associated with increased amount of α-Al dendrites has contributed to the increasing of damping capacity [3, 11].

1.1. Dynamic mechanical properties

Damping capacity (tan ϕ) is a measure of a material's ability to dissipate elastic strain energy during mechanical vibration or wave propagation [12, 13]. The damping capacity of structural material has been recognized as one of significant factors in material selection [14].

In an ideally elastic material, $\phi = 0$ and $\sigma/\varepsilon = E$, the Young's modulus. However, most materials are inelastic owing to some energy dissipation, which occurs in the same frequency range as the imposed stress,

*Corresponding author: tel.: +6 (04) 979 8619; fax: +6 (04) 979 8178; e-mail address: mazlee@unimap.edu.my

therefore the strain lags behind the stress and ϕ is not zero. The ratio of σ/ε is the complex modulus, E^*, and is defined as

$$E^* = E' + \mathrm{i}E'', \tag{1}$$

where E' and E'' are the components of E^* and are known as the storage modulus and loss modulus, respectively. The ratio of two elastic moduli $E''/E' = \tan\phi$ is the damping capacity of the material. This term is dimensionless and shows the ratio of energy lost (dissipated by heat) per cycle to the energy stored [15].

Only few studies are conducted on damping of Al-Si based alloys. Yijie et al. [3, 11] found the increment of damping capacity by the grain refinement with the addition of nano grain refiner in A356 alloy. According to Zhou et al. [14], the improvement of damping was linked with dislocation movements induced by the thermal stresses due to the coefficient of thermal expansion mismatch between the Al matrix and Si particles in Al-11.8Si alloy. Meanwhile Lee [16] reported that the maximum specific damping capacity coincided with the maximum age hardening condition but simultaneously decreased with overaging in Al-7Si-0.3Mg alloy with T6 treatment. This paper presents the results of an investigation of the effects of melt superheat treatment on the microstructure and dynamic mechanical properties of A357 alloys.

2. Experimental

The raw material used as a matrix alloy in this research work was primary cast ingot Al-Si-Mg alloy (abbreviated as cast ingot) supplied by National Center for Machinery & Tooling Technology (NCMTT), SIRIM Berhad, Malaysia. The alloy had been cast by continuous casting process and was delivered in the form of bar. The chemical composition of cast alloy was analyzed using arc spark spectroscopy (SPECTROMAX, Germany) and the composition was complied with A357 alloy. Table 1 shows the chemical composition of primary cast ingot A357 alloy.

The cast ingot was melted in crucibles by using electric furnace. Prior to casting to form superheated A357 alloy, the cast ingot was prepared by heating up to the melt superheat temperature of 900 °C for 1 hour. The 314 stainless steel mold was preheated at 250 °C for 1 hour. The superheated A357 alloy was produced by pouring the molten cast ingot into the 314 stainless steel mold at 700 °C via conventional gravity casting technique. The non-superheated A357 alloy was also fabricated using the same parameters except the heating to the melt nonsuperheat temperature of 750 °C for 1 hour prior to casting process.

The microstructures of all the specimens were characterized by light microscope. Specimens were prepared by the standard metallography methods of cutting and mounting followed by wet grinding on a series of SiC papers. Finally, the specimens were polished with 6 μm, 3 μm and 1 μm diamond suspension using Naples cloth. The etchant used was 0.5 % HF in order to reveal the morphologies of α-Al dendrites and eutectic Si particles in the microstructures.

Table 1. Chemical compositions of primary cast ingot A357

Elements	Si	Mg	Fe	Mn	Ti	Al
Composition (wt.%)	7.24	0.54	0.12	<0.10	0.10	balance

A dynamic mechanical analyzer (Pyris Diamond DMA model, USA) was used to measure storage modulus, loss modulus and damping capacity. Dynamic mechanical analysis was carried out in the three point bending mode using a dual cantilever system. The composite specimens were prepared in the form of rectangular bars with dimensions of 50 × 10 × 1.0 mm^3. The tested specimens were run at 2 °C min^{-1} heating rate from 30 to 400 °C with 100 μm strain at 10 Hz in a flowing purified nitrogen gas.

Differential scanning calorimetry (DSC) studies were carried out on the specimens of non-superheated and superheated as-cast A357 alloy specimens using DSC Q10 TA Instrument model. Parallel slices 0.5 mm thick were cut from the specimens using precision diamond blade and discs about 5 mm in diameter were then punched from the slices. The specimens were tested at 10 °C min^{-1} heating rate from 50 to 450 °C.

3. Results and discussion

3.1. Microstructure

Figures 1 and 2 show the microstructure of non-superheated and superheated A357 alloys, respectively. Generally, both as-cast alloy microstructures showed the presence of α-Al dendrites and eutectic Si particles. Figure 1a shows the existence of coarser and angular eutectic Si particles surrounded with larger α-Al dendrites in non-superheated A357 alloy. The irregular and non-equiaxed α-Al dendrites of about 150 μm size were also observed in this alloy. These features were attributed to the slow solidification rate during casting. Figure 1b illustrates the coarse interdendritic of eutectic Si particles of about more than 10 μm size which segregated within the α-Al dendrites structure.

In Fig. 2a, a mixture of finer about 100 μm size and rounded eutectic Si particles and also preferably oriented α-Al dendrites are observed in superheated

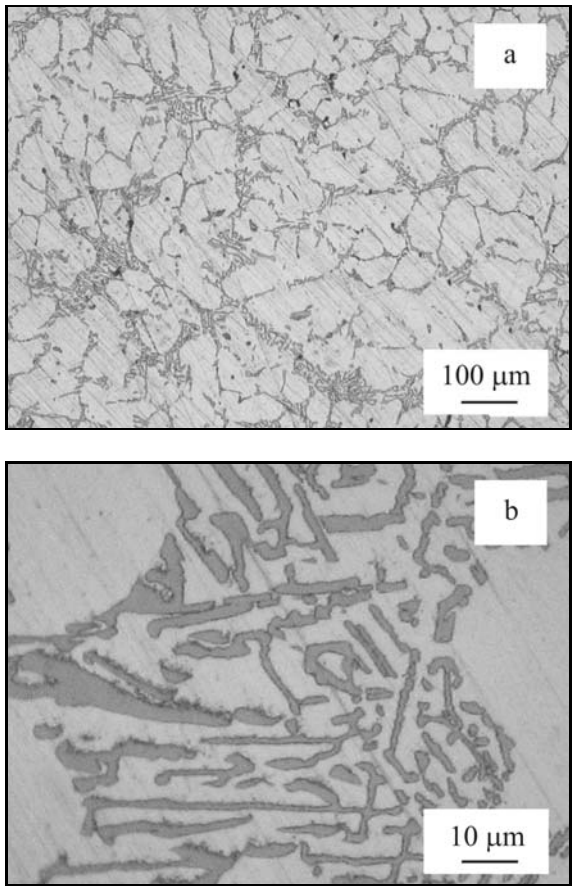

Fig. 1. Optical microstructure of non-superheated A357 alloy: (a) at low magnification (100×), (b) at high magnification (2000×).

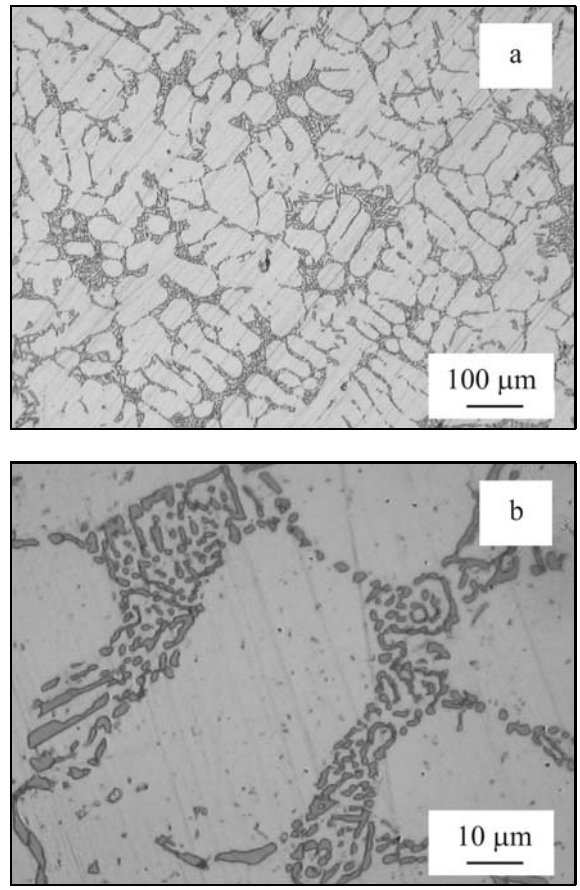

Fig. 2. Optical microstructure of superheated A357 alloy: (a) at low magnification (100×), (b) at high magnification (2000×).

A357 alloy. It is believed that the melt superheat prior to casting has influenced the microstructure. A high superheat treatment temperature of 900 ℃ has also assisted the degeneration of Si atom clusters. It was found also that superheat treatment in the current research tended to refine the eutectic Si particles and changed the shape of α-Al dendrite to finer, rounded and preferably oriented α-Al dendritic structures.

The finer interdendritic of eutectic Si particles of about less than 10 μm are found to be segregated and agglomerated within the α-Al dendrites as shown in Fig. 2b. According to Wanqi et al. [17], if the superheat temperature is kept below 800 ℃, there is no obvious effect on the refinement of the Si particles in A356 alloy. However, over 800 ℃, the Si particles are significantly refined. At melt temperatures of 900 ℃, the refinement of the Si particles by melt superheat is nearly comparable to that obtained with 0.01 percent Sr addition. Wanqi et al. [17] contributed this refinement effect of superheat to the existence of Mg in the A356 alloy, as they did not find any such effect in Al-Si binary alloys that contained no Mg.

3.2. Dynamic mechanical properties

Figures 3, 4 and 5 show the dynamic mechanical properties behavior of non-superheated and superheated A357 alloy in terms of storage modulus, loss modulus and damping capacity at 10 Hz frequency, respectively. They show a general phenomenon of progressively decreasing storage moduli with increasing temperature (Fig. 3). In contrast, the loss moduli and damping capacity generally increase with increasing temperature (Figs. 4 and 5). It can be seen that the storage moduli, loss moduli and damping capacity are sensitive to the processing method of the alloys and testing temperature range.

The higher storage modulus in superheated A357 alloy is attributed to the combined effect of finer and rounded interdendritic eutectic Si particles together with smaller and preferably oriented α-Al dendrites compared to coarser and angular interdendritic eutectic Si particles and larger α-Al dendrites in non-superheated A357 alloy. Preferably oriented α-Al dendrites have a profound effect to influence the en-

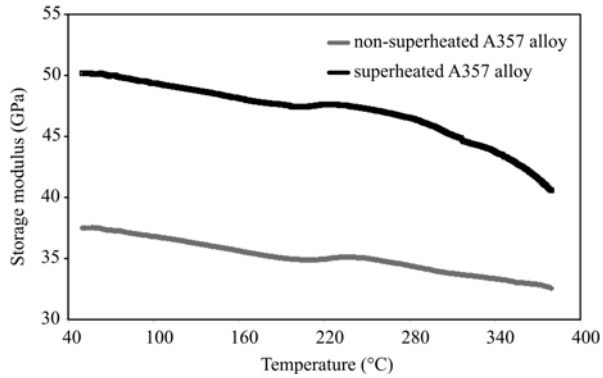

Fig. 3. The relationship of storage modulus and elevated temperatures of non-superheated and superheated A357 alloys.

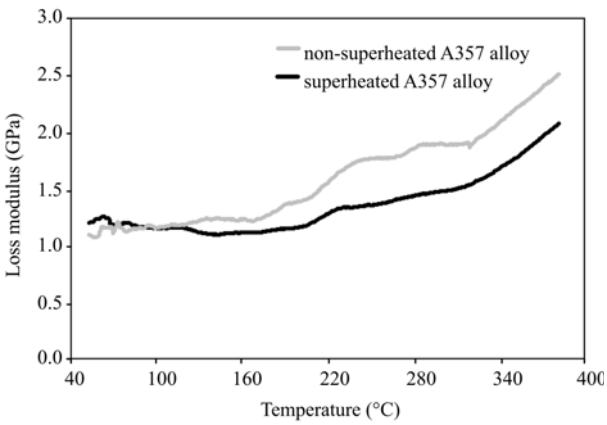

Fig. 4. The relationship of loss modulus and elevated temperatures of non-superheated and superheated A357 alloys.

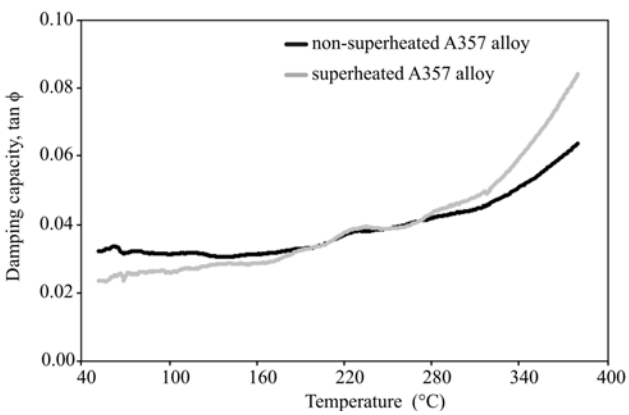

Fig. 5. The relationship of damping capacity modulus and elevated temperatures of non-superheated and superheated A357 alloys.

hancement of storage modulus as reported by textured structure [15].

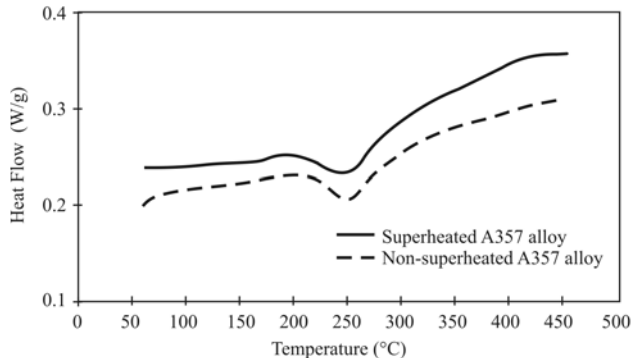

Fig. 6. The DSC thermographs of non-superheated and superheated A357 alloys.

The eutectic Si particles morphology has been found to play a vital role in determining the mechanical properties. Particle size, shape and spacing are factors that characterize Si morphology. A prolonged solution treatment on a cast Al-Si-Mg alloy has produced the spheroidized Si particles that contributed to the better tensile strength and elongation [18]. Ogris et al. [19] reported that eutectic silicon spheroidization treatment results in outstanding fracture elongation values (up to 18 percent) at good yield strength level ($\sim$ 230 MPa) in Al-Si alloys.

The loss moduli trend of superheated A357 alloy specimen in Fig. 4 has shown more efficient energy loss relatively due to finer and rounded interdendritic eutectic Si particles and combined structure of smaller and preferably oriented α-Al dendrites. The refinement of eutectic Si particles along with smaller α-Al dendrites play a partial role on the dissipation of elastic strain energy, as reported by Zhang et al. [3].

It is expected that coarser α-Al dendrites in non-superheated A357 alloy (150 µm) have generated more dislocations compared to finer α-Al dendrites in superheated A357 alloy (100 µm). Dislocation plays a significant role in the damping capacity of non-superheated A357 alloy and subsequently was higher than superheated A357 alloy in lower temperatures range of 50 to 190 °C.

Figure 6 has demonstrated the differential scanning calorimetry (DSC) thermographs of superheated and non-superheated A357 alloys at elevated temperatures, respectively. It can be noted that the damping capacity trend line of both alloys has overlapped between 190 to 277 °C. The overlap of damping capacity trend lines has resembled the obvious area changes under DSC thermographs in Fig. 6. The damping capacities for both alloys were almost the same values in middle temperature range of 190 to 277 °C, which was believed due to the balance between dislocation and precipitation damping mechanisms. Meanwhile, at high temperature range of 278 to 380 °C, the effect of size reduction of α-Al dendrites and refinement of

eutectic Si particles play a significant role in the improvement of damping capacity of superheated A357 alloy as also observed above 275 ℃ in refined A356 alloy by Yijie et al. [11].

It has been reported that, above 400 ℃, the damping capacity will reach the maximum peak. A prior work by Elomari et al. [20] has led to the conclusion that the mechanism responsible for the damping peak is probably related to the transformation processes (growth of precipitates) in the material. Presumably, the effect of superheating has accelerated the precipitation process at 278 ℃ to 380 ℃.

Unequiaxed structure of α-Al dendrites in non-superheated and superheated A357 alloys, respectively, has contributed to the uneven trend lines of damping capacity as illustrated in Fig. 5. This finding was dissimilar to the smooth trend line of equiaxed grain, as was observed by Zhang et al. [21].

3.3. Damping mechanisms

3.3.1. Dislocation damping

Dislocation damping is noteworthy because it plays a critical role, not only in the damping response of crystalline material, but also in the overall mechanical behavior of the materials [21]. According to Granato-Lücke theory [22, 23], the dislocation structure is assumed to consist of segments of length L_N along which weak pinning points are distributed randomly, the dislocations are pinned by the fine precipitation.

At low temperatures, dislocations can only drag the weak pinning points such as some solute atoms and vacancies to move, and then dissipate energy. At elevated temperatures, the stress for breakaway from the weak pinning points is decreased because the process is thermally activated [24]. Therefore, above certain temperatures, dislocations would move faster and then break away dramatically from the weak pinning points. It would then become a long dislocation in the condition of hard pinning such as network node of dislocation and in second phase, the energy dissipated by dislocation motion would not increase, and thus the damping capacity values might decrease slightly. Consequently, a damping peak is caused. Afterwards, the damping capacity may increase again due to the appropriate damping mechanism at elevated temperatures.

The interface between particles and matrix is a fundamental parameter of all micro heterogeneous materials, especially to derive the properties of these materials from, and it depends upon the transfer of load from the matrix to the reinforcing second phase. Consequently, in the past, important efforts have been invested on the one hand to characterize the interfaces, and on the other hand to establish the role of the mismatch between the coefficients of thermal expansion (CTE) of particles and matrix on the mechanical behavior of the composite [25]. However, Zhou et al. [14] reported that the study of Al-Si alloys in dependence on temperature had shown that an important contribution to damping was linked with dislocation movements induced by the thermal stresses due to the CTE mismatch between the aluminum matrix and silicon particles.

In present research, Fig. 5 shows one temperature peak at about 235 ℃ before the damping capacity of non-superheated and superheated A357 alloys starts to deviate above 277 ℃. It is indicated that the temperature peak is attributed to the dislocation vibration within the Si particles. The same temperature peak has been observed at relatively lower temperatures in cast iron due to the dislocation vibration within the graphite inclusions [26]. So, it can be proposed that dislocation damping is the mechanism for non-superheated and superheated A357 alloys at lower temperatures (50 to 277 ℃).

3.3.2. Grain boundary damping

Grain boundary sliding is another mechanism giving rise to damping behavior. Grain boundary damping which is associated with grain boundary relaxation, inelasticity or viscosity in polycrystalline metals has been studied by Kê [27] and Zener [28]. In polycrystalline metals, the grain boundaries display viscous like properties. The viscous flow at grain boundaries will convert mechanical energy produced under cyclic shear stress into thermal energy as a result of internal friction at grain boundaries. The thermal energy will then be dissipated by the conductivity of the metal and heat exchange with the surroundings. The energy absorbed at grain boundaries is dependent on the magnitude of the shear stress and the grain boundary area per unit volume, i.e. grain size.

Kê [27] reported that a polycrystalline aluminum showed higher damping compared to single crystal aluminum. The difference in grain boundary damping between the polycrystalline aluminum and the single crystal aluminum became manifest when the testing temperature exceeded 200 ℃. In present study, a significant difference between the damping capacity of non-superheated and superheated A357 alloys above 277 ℃ is illustrated in Fig. 5. Therefore, grain boundary damping is the most reliable damping mechanism for non-superheated and superheated A357 alloys at the elevated temperatures (278 to 380 ℃).

4. Conclusions

Improvement in damping capacity at lower temperatures in non-superheated A357 alloy has been attributed by more generated dislocations in coarser

α-Al dendrites. Meanwhile, refinement of eutectic Si particles and smaller α-Al dendrites via superheat treatment has been contributed to the enhancement in damping capacity at elevated temperatures in superheated A357 alloy. Generally, the damping mechanisms in non-superheated and superheated A357 alloys ascribed to be a combination of dislocation damping at lower temperatures (50 to 277 ℃) and grain boundary damping at elevated temperatures (278 to 380 ℃).

Acknowledgements

The authors are grateful to UniMAP for the financial support under Short Term Grant (Acc. no: 9003-00021).

References

[1] SHIVKUMAR, S.—WANG, L.—APELIAN, D.: J. Metals, *43*, 1991, p. 26.
[2] DJURDJEVIC, M.—STOCKWELL, T.—SOKOLOWSKI, J.: Int. Cast. Metall. J., *12*, 1999, p. 67.
[3] YIJIE, Z.—NAIHENG, M.—YONGKANG, L.—SONGCHUN, L.—HAOWEI, W.: Mater. Lett., *59*, 2005, p. 2174.
[4] WANG, Q. G.—DAVIDSON, C. J.: J. Mater. Sci., *36*, 2001, p. 739. doi:10.1023/A:1004801327556
[5] CHEN, Z. W.—QI, J. W.—JIE, Z. R.: Mater. Lett., *59*, 2005, p. 2183.
[6] HAQUE, M. M.—AHMAD ISMAIL, F.: J. Mater. Proc. Technol., *162–163*, 2005, p. 312. doi:10.1016/j.jmatprotec.2005.02.049
[7] QIU, D.—ZHANG, M. X.—TAYLOR, J. A.—FU, H. M.—KELLY, P. M.: Acta Mater., *55*, 2007, p. 1863. doi:10.1016/j.actamat.2006.10.047
[8] GU, Z. H.—WANG, H. Y.—ZHENG, N.—ZHA, M.—JIANG, L. L.—WANG, W.—JIANG, Q. C.: J. Mater. Sci., *43*, 2008, p. 980. doi:10.1007/s10853-007-2275-5
[9] WANG, J.—HE, S.—SUN, B.—LI, K.—SHU, D.—ZHOU, Y.: Mater. Sci. Eng., *A338*, 2002, p. 101. doi:10.1016/S0921-5093(02)00067-9
[10] BASAVAKUMAR, K. G.—MUKUNDA, P. G.—CHAKRABORTY, M.: Bull. Mater. Sci., *30*, 2007, p. 439. doi:10.1007/s12034-007-0070-1
[11] YIJIE, Z.—NAIHENG, M.—HAOWEI, W.—XIANFENG, L.: Mater. Design, *3*, 2008, p. 706.
[12] BAIK, K. H.—PATRICK, S. G.: Mater. Sci. Eng. A, *265*, 1999, p. 77. doi:10.1016/S0921-5093(99)00014-3
[13] AGARWALA, V.—SATYANARAYANA, K. G.—AGARWALA, R. C.: Mater. Sci. Eng., *A270*, 1999, p. 210. doi:10.1016/S0921-5093(99)00251-8
[14] ZHOU, X.—FOUGĚRES, R.—VINCENT, A.: J. Phys. III France, *2*, 1992, p. 2185. doi:10.1051/jp3:1992240
[15] SHAMSUL, J. B.—HAMMOND, C.—COCHRANE, R. F.: Mater. Sci. Technol. A, *14*, 1998, p. 1075.
[16] LEE, C. D.: Mater. Sci. Eng. A, *394*, 2005, p. 112. doi:10.1016/j.msea.2004.11.033
[17] WANQI, J.—HONGWEI, C.—REIF, W.—MÜLLER, K.: Metall. Mater. Trans., *34A*, 2003, p. 799.
[18] ABOU EL-KHAIR, M. T.: Mater. Lett., *59*, 2005, p. 894. doi:10.1016/j.matlet.2004.11.041
[19] OGRIS, E.—WAHLEN, A.—LÜCHINGER, H.—UGGOWITZER, P. J.: J. Light Met., *2*, 2002, p. 263. doi:10.1016/S1471-5317(03)00010-5
[20] ELOMARI, S.—BOUKHILI, R.—SKIBO, M. D.—MASOUNAVE, J.: J. Mater. Sci., *30*, 1995, p. 3037. doi:10.1007/BF01209214
[21] ZHANG, J.—PEREZ, R. J.—GUPTA, M.—LAVERNIA, E. J.: Scr. Metall. et. Mater., *28*, 1993, p. 91. doi:10.1016/0956-716X(93)90543-2
[22] GRANATO, A. V.—LÜCKE, K.: J. Appl. Phys., *27*, 1956, p. 583. doi:10.1063/1.1722436
[23] GRANATO, A. V.—LÜCKE, K.: Appl. Phys., *27*, 1956, p. 789.
[24] GRANATO, A. V.—LÜCKE, K.: J. Appl. Phys., *52*, 1981, p. 7136. doi:10.1063/1.328687
[25] WITHERS, P. J.—STOBBS, W. M.—PEDERSEN, O. B.: Acta Metall., *37*, 1989, p. 3061. doi:10.1016/0001-6160(89)90341-6
[26] XINBAO, L.—SUSUMU, T.—YOSHIAKI, O.—FUXING, Y.: J. Mater. Sci., *40*, 2005, p. 1773.
[27] KÊ, T. S.: Phys. Rev., *72*, 1947, p. 41. doi:10.1103/PhysRev.72.41
[28] ZENER, C.: Elasticity and Anelasticity in Metals. Chicago, University of Chicago Press 1948.